

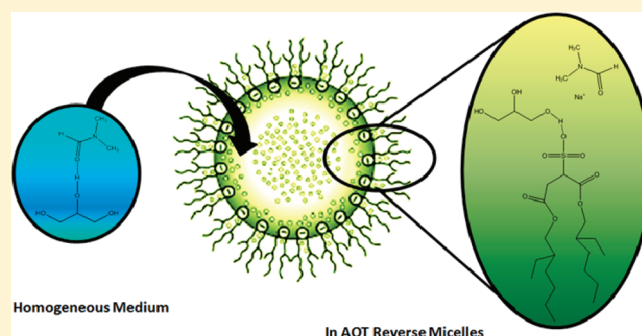
A New Organized Media: Glycerol:*N,N*-Dimethylformamide Mixtures/AOT/*n*-Heptane Reversed Micelles. The Effect of Confinement on Preferential Solvation

Andrés M. Durantini, R. Dario Falcone, Juana J. Silber, and N. Mariano Correa*

Departamento de Química, Universidad Nacional de Río Cuarto, Agencia Postal # 3, C.P. X5804BYA Río Cuarto, Argentina

S Supporting Information

ABSTRACT: In this work we investigate the behavior of the glycerol (GY):*N,N*-dimethylformamide (DMF) mixture in homogeneous and sodium 1,4-bis(2-ethylhexyl)sulfosuccinate (AOT)/*n*-heptane reversed micelles (RMs) media. To achieve this goal we have used the solvatochromic behavior of 1-methyl-8-oxyquinolinium betaine (QB) as an absorption probe, and dynamic light scattering (DLS). QB shows strong preferential solvation when it is dissolved in the GY:DMF mixture, and, as QB is a good hydrogen bond acceptor molecular probe, it is preferentially solvated by the GY–DMF hydrogen-bonded (H-bonded) species. On the other hand, when the GY:DMF mixture was investigated in AOT RMs, the results show that the mixture is encapsulated in the polar core of the AOT RMs. DLS confirms the formation of the GY:DMF/AOT/*n*-heptane RMs since an increase in the $W_s = ([GY] + [DMF])/[AOT]$ values causes an increment in the RMs droplets sizes. The solvatochromic behavior of QB, which resides at the AOT RMs interface, shows that QB is mostly solvated by GY molecules, especially at low W_s values. Thus, it seems that upon encapsulation inside the polar core of the AOT RMs, the GY–DMF interaction diminishes due to the strong AOT–GY interaction. ^1H NMR chemical shifts of GY and DMF measured in the different AOT RMs investigated shows that GY and DMF behave practically as noninteracting solvents inside the RMs.



INTRODUCTION

Reversed micelles (RMs) are the aggregates of surfactants formed in a nonpolar solvent, in which the polar head groups of the surfactants point inward and the hydrocarbon chains point toward the nonpolar medium.^{1–3} A widespread surfactant used to form RMs is the sodium 1,4-bis(2-ethylhexyl)sulfosuccinate (AOT; see Scheme 1) because the micelles formed with this surfactant can solubilize a large quantity of water in a nonpolar solvent.^{1–3}

Besides water, some polar organic solvents, having high dielectric constants and very low solubility in hydrocarbon solvents, can also be encapsulated in RMs.⁴ The most common polar solvents used include formamide (FA), dimethylformamide (DMF), dimethylacetamide (DMA), ethylene glycol (EG), propylene glycol (PG), and glycerol (GY).^{5–31} The AOT/*n*-heptane RMs containing these solvents are known to be spherical, and it has been demonstrated that the size of the RMs depends on the $W_s = [\text{polar solvents}]/[\text{AOT}]$ values.^{6,21}

Regarding other physicochemical properties of the nonaqueous RMs, different studies have shown that the polar solvents, when restricted to the nanometer-scale core of the aggregates, behave differently from the bulk solvents as a result of the specific interactions and confined geometries.^{14–20} For example, Fourier transform infrared (FT-IR)^{10,16,18,20} and ^1H NMR^{16,18} spectroscopy

have shown that GY and EG interact with the AOT polar head through hydrogen bond (H-bond) interactions that maintain the typical spherical RMs structure but break the solvent H-bond structure present in the bulk.^{6,14,16,17}

We have recently demonstrated using FT-IR technique³⁰ that GY interacts through a H-bond with the AOT SO_3^- group at the interface remaining in the polar core of the micelles, while DMF encapsulated inside the AOT RMs interacts with the Na^+ counterions and not with the C=O nor the SO_3^- AOT groups. Thus, the weakly associated bulk structure of DMF is broken inside AOT RMs because the interactions with the Na^+ counterions. Also, in a recent communication³¹ we have shown using dynamic light scattering (DLS) that water, GY, EG, DMF, DMA, or FA/AOT/*n*-heptane RMs droplet sizes depend on the different polar solvents–AOT interactions and not on their molar volume, V_m .

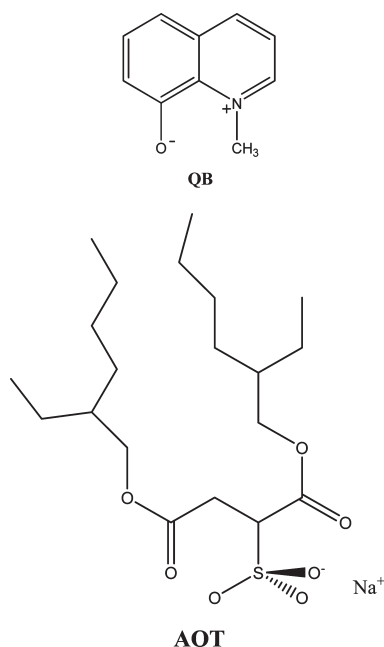
The study of H-bond molecular interactions of binary mixtures containing glass-forming liquid solvents is currently a significant challenge in the research of soft condensed matter science because of their wide applications in the field of science

Received: December 30, 2010

Revised: April 6, 2011

Published: April 25, 2011

Scheme 1. Molecular Structure of the Molecular Probe Used: QB and the AOT Surfactant



and technology.³² As a result of the intermolecular interactions, preferential solvation of solutes in mixed solvents may be observed. This term applies if the local mole fractions of the solvent components in a solvation microsphere surrounding the solute differ from the bulk ones.^{33–35}

As it is well-known, several biological phenomena occur at interfaces rather than in homogeneous solution. In particular, interface/protein interactions play a key role in reactions involving membrane bound proteins and also in the H-bond interactions between water and other polyols and peptides compounds.³⁶ In this sense, even when RM constitutes an oversimplified model, the very large interfacial region provided by these systems can be expected to enhance some effects, such as H-bond interactions between peptide bonds of globular proteins, due to the fact that in these media the amphipathic essence of a biological membrane is preserved.^{37,38} We have demonstrated that the superactivity of α -chymotrypsin encapsulated in RMs depend strongly on the H-bond ability of the media. The encapsulation of the globular enzyme was confirmed using DLS.^{37,39}

GY is a polyol that stabilizes biological molecules like proteins and enzymes in water^{40–42} and in AOT RMs.³⁷ Among different amides, DMF is of particular interest in view of the lack of H-bonding in the bulk solvent and of the structure alteration of its aqueous mixtures.⁴³ Also, DMF is one of the most important aprotic organic solvents largely used in analytical and electrochemical applications. Furthermore, as the interactions between hydroxyl and amide groups play an important role in the solvation of peptides,³³ the amide group can serve as a model of the peptide bond, and DMF can serve as a model compound for peptides to obtain information on protein systems.⁴⁰

Despite the good numbers of studies performed in nonaqueous RMs that encapsulates single polar solvents in the RMs polar core, the behavior of nonaqueous solvents mixture upon encapsulation is not known. With this background and in the context of our studies in nonaqueous RMs, we consider it worthy

to investigate the effect that the confinement has on the interaction between two very interacting solvents: the strong H-bond donor, GY, and the strong H-bond acceptor, DMF.^{32,40,43} In addition, we are interested in the nonaqueous RMs interface properties when the GY:DMF mixture is encapsulated in the polar core of the RMs. Thus, in this work we investigate the interactions between GY and DMF in homogeneous and in nonaqueous AOT/*n*-heptane RMs to gain insights on how the constrained medium affects the GY–DMF interaction creating a unique microenvironment. To achieve this goal, we have used the solvatochromic behavior of the molecular probe 1-methyl-8-quinolinium betaine (QB, Scheme 1) because its absorption spectrum is highly sensitive to its local environment.^{44–46} We also use DLS to demonstrate that the AOT RMs are effectively formed. Our interpretation of the data suggests that in homogeneous media GY and DMF interact strongly through H-bond interaction, while, encapsulated in the polar interior of the AOT RMs, the GY–DMF interaction diminishes since GY molecules interact strongly with the AOT polar head. Two unique effects can be found upon the mixture confinement: the QB preferential solvation is noticeably changed, and the GY–AOT interactions seem to control the RMs droplet size.

EXPERIMENTAL SECTION

Materials. GY and DMF from Aldrich (high-performance liquid chromatography (HPLC) grade) were used without further purification. *n*-Heptane (Merck HPLC quality) was used as received.

AOT was dried under reduced pressure, over P₂O₅ until constant weight. The UV–vis spectra of QB (a solvatochromic probe) in the presence of AOT RMs showed that the surfactant is free of acidic impurities, which would have greatly reduced the intensity of the solvatochromic B₁ band at 502 nm.^{45,46} QB was synthesized by a procedure reported previously.⁴⁴

Methods. The GY–DMF solutions at any GY bulk mole fraction (X_{GY}^0) value composition studied were prepared by weight.

The stock solutions of AOT in *n*-heptane were prepared by weight and volumetric dilution. To obtain optically clear solutions, they were shaken in a sonicating bath, and the polar solvents were added using a calibrated microsyringe. The surfactant solution was 0.10 M in *n*-heptane. For any X_{GY}^0 value studied, the amount of polar solvents present in the system is expressed as the molar ratio between the total polar solvents amount and the AOT concentration $W_s = ([GY] + [DMF])/[AOT]$. The lowest value for W_s ($W_s = 0$) corresponds to a system without the addition of the polar solvents.

To introduce the probe, a 0.01 M solution of QB was prepared in methanol (Sintorgan HPLC quality). The appropriate amount of this solution to obtain a given concentration of the probe in the homogeneous or micellar medium was transferred into a volumetric flask, and the methanol was evaporated by bubbling dry N₂; then, the suitable GY–DMF mixtures or the AOT RMs solution was added to the residue.

UV/visible spectra were recorded using a spectrophotometer Shimadzu 2401 with a thermostatted sample holder. The path length used in absorption experiments was 1 cm. All experimental points were measured three times with different prepared samples. The pooled standard deviation was less than 5%. All the experiments were carried out at 25 ± 0.5 °C.

The diameters of the different nonaqueous AOT RMs were determined by DLS (Malvern 4700 with goniometer and 7132

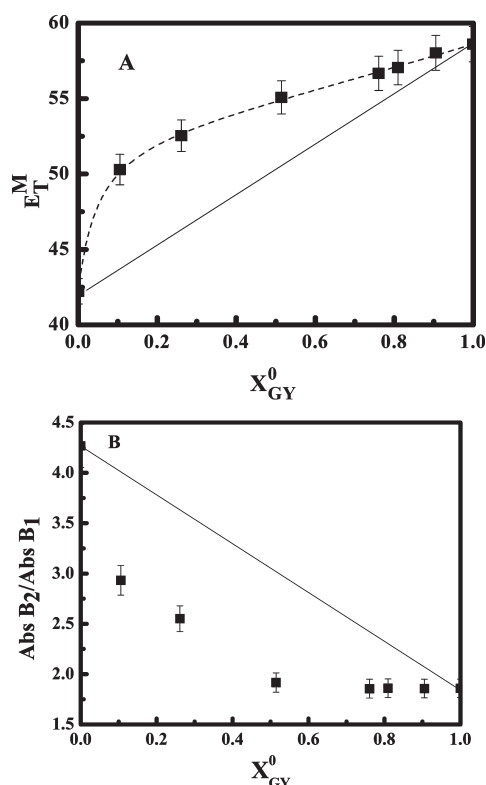


Figure 1. (A) $E_T(30)$ values for QB in the GY:DMF mixture (E_T^M) at different X_{GY}^0 : (■) experimental points, (----) curve fitted with eq 11. (B) $Abs B_2/Abs B_1$ ratio values as a function of X_{GY}^0 for QB in the GY:DMF mixture. $[QB] = 1 \times 10^{-4}$ M. The straight line was plotted to guide the eye; it represents no preferential solvation of QB by the mixture.

correlator) with an argon-ion laser operating at 488 nm. Multiple samples at each size were made, and 30 independent size measurements were made for each individual sample at the scattering angle of 90°. The algorithm used was CONTIN, and the DLS experiments show that the polydispersity of the nonaqueous AOT RMs size is less than 5%. All the experiments were carried out at 25 ± 0.5 °C.

For the ¹H NMR experiments, a Bruker 200 NMR spectrometer was used. The spectrometer probe temperature (25 °C) was periodically monitored by measuring the chemical shift difference values between the two singlets of a methanol reference sample, which is well-known to depend on the temperature.¹⁸ The probe thermal stability was assured by the observation that successive measurements of the sample chemical shift (after 10 min in the probe for thermal equilibration) were within digital resolution limit. A capillary tube containing D₂O was used as a frequency “lock”. Chemical shifts were measured relative to internal TMS, and chemical shifts were reproducible within 0.01 ppm.

RESULTS AND DISCUSSION

QB in GY:DMF Homogeneous Mixtures. The QB absorption spectra in the GY:DMF binary mixtures at different X_{GY}^0 are shown in Figure S1, in the Supporting Information. As it can be seen, QB presents two electronic absorption bands B_1 and B_2 , which sense different effects as we have previously demonstrated.^{45,46} The band in the visible region, B_1 , is due to the transition from a predominantly dipolar ground state to an excited

state of considerably reduced polarity. It was found that the B_1 solvatochromism is mainly due to the polarity/polarizability ability of the medium. However, this band also correlates with the H-bond donor ability of the medium.⁴⁵ With increasing the polarity and/or the H-bond donor ability of the solvent, the ground state becomes more stable, which leads to an increase in the transition energy, i.e., negative solvatochromism. The transition energy (expressed in kcal mol⁻¹) of QB can be used as a polarity parameter, E_{QB} , similar to Dimroth et al.'s $E_T(30)$ value⁴⁷ because it has been demonstrated that the E_{QB} value correlates in a linear relationship with this solvent parameters through eq 1.⁴⁴

$$E_T(30) = 1.71E_{QB} - 49.1 \quad (1)$$

The band in the UV region, B_2 , which was assigned to a charge transfer from the phenoxide ion to the aromatic ring (Scheme 1), also shifts hypsochromically with the polarity of the solvent, although in lesser magnitude than the visible band.⁴⁵ Moreover, it was demonstrated that the B_2 band frequency is also sensitive to the H-bond donor capability of the solvent.⁴⁵ Interestingly, the absorbance ratio of both bands ($Abs B_2/Abs B_1$) is only sensitive to the H-bond ability of the medium.⁴⁵ $Abs B_2/Abs B_1$ value is large for solvents with low H-bond ability and decreases as the solvent H-bond capability increases. Consequently, the $Abs B_2/Abs B_1$ ratio is used in combination with the absorption bands shifts to determine the properties of the microenvironment surrounding the probe.^{45,46}

Figure 1 A shows the plot of the $E_T(30)$ values defined as E_T^M parameter and obtained through eq 1,⁴⁴ for the GY:DMF binary mixture as a function of the GY bulk mole fraction, X_{GY}^0 . As it can be observed, the experimental points deviate from linearity in the whole X_{GY}^0 range studied and also shows a dramatic increase of the E_T^M values with the increasing proportion of GY until a X_{GY}^0 around 0.5 (but never higher than the GY's $E_T(30)$ value⁴⁸). After that, the values remain almost constant and similar to the value obtained in GY pure solvent. The solute surrounds itself preferably by the component in the mixture, which leads to the more negative Gibbs energy of solvation, as expected.⁴⁹ The observation that the solvent shell has a composition other than the macroscopic ratio is termed selective or preferential solvation.^{33,35} Thus, QB seems to detect more GY molecules in its solvent shell than that corresponding to the bulk composition, and probably as a consequence the GY:DMF mixture is not ideal as it was previously demonstrated by other authors.^{32,40,43,50}

A question may arise here about why QB, being soluble in both pure solvents, DMF and GY, prefers to be solvated by GY molecules when QB is dissolved in the GY:DMF mixture. In this sense, it should be taken into account that the solute preferential solvation is produced not only by nonspecific interactions but also by specific interactions such as by H-bond formation between the solute and the solvent molecules.⁴⁹ As QB is a molecular probe that can specifically detect H-bond interactions with its microenvironment through its $Abs B_2/Abs B_1$ ratio values,⁴⁵ we attempt to elucidate the origin of the QB preferential solvation in the GY:DMF mixture, plotting the $Abs B_2/Abs B_1$ ratio versus X_{GY}^0 (Figure 1 B). It can be observed that the absorbance ratio values also strongly deviate from the linearity in the whole composition mixture studied. Moreover, the $Abs B_2/Abs B_1$ ratio values dramatically decrease up to an X_{GY}^0 value of ~ 0.5 , demonstrating that H-bond interactions play a crucial role in the QB's preferential solvation in the GY:DMF mixture. It is

known that the GY:DMF mixtures are not ideal due to strong H-bond interactions between GY and DMF. Moreover, the predominance of the formation of hydrogen bonds between DMF and GY through $\text{C}=\text{O}\cdots\text{H}-\text{O}$ favors the rupture of H-bonding between GY–GY.⁴⁰ Probably, as it has been demonstrated, the aprotic dipolar behavior of DMF molecules significantly changes the ordering of the H-bonded networks of pure GY.³² Thus, it seems that the GY:DMF H-bonded species make stronger H-bond interactions with the QB molecules than GY alone.

In order to understand and quantify how the solvent mixtures influence the QB behavior, one should know the composition that the probe “feels”, that is, the composition in its immediate vicinity. This is, as discussed earlier, different from the bulk composition of the mixed solvent.³⁴ Moreover, when solvent–solvent specific interactions in the mixture are possible, the mixtures do not behave as ideal solutions. Then, both solute–solvent and solvent–solvent interactions have been found to play significant roles in the preferential solvation characteristics.³⁴

As the B_1 frequency values is mainly sensitive to the polarity of the medium, and the $\text{Abs}B_2/\text{Abs}B_1$ ratio is only sensitive to the H-bond donor ability of the solvent (specific interaction),⁴⁵ we can use both parameters in order to quantify the preferential solvation around QB.

Considering that the solvation shell obeys the regular solution laws, it is possible to quantify the preferential solvation as follows:³⁴ we may calculate the set of local mole fractions considering that the QB ν_{max} value in the GY:DMF mixtures can be expressed as eq 2:

$$\nu_{\text{M}} = X_{\text{GY}}^{\text{S}}\nu_{\text{GY}} + X_{\text{DMF}}^{\text{S}}\nu_{\text{DMF}} \quad (2)$$

where ν_{M} is the frequency of the QB B_1 maximum absorbance band in the GY:DMF mixture, X_{GY}^{S} and $X_{\text{DMF}}^{\text{S}}$ are the solvent compositions in molar fractions in the immediate neighborhood, the primary solvation shell of QB,³⁵ and ν_{GY} and ν_{DMF} are the frequencies of the QB B_1 maximum absorbance band in pure GY and DMF, respectively. It should be taken into account that eq 2 predicts a straight line for the plot of ν_{M} as a function of X_{GY}^{S} or $X_{\text{DMF}}^{\text{S}}$ only if the primary solvation shell of QB has the same composition as the bulk solvent mixture (X_{GY}^{0} and $X_{\text{DMF}}^{\text{0}}$). Clearly this is not the case for QB in the GY:DMF mixture as Figure 1 shows.

Hence, the GY composition, X_{GY}^{S} , can be calculated by eq 3:

$$X_{\text{GY}}^{\text{S}} = \frac{(\nu_{\text{M}} - \nu_{\text{DMF}})}{(\nu_{\text{GY}} - \nu_{\text{DMF}})} \quad (3)$$

A parameter, Δ ,^{34,51} which can be used to quantify the extent of the preferential solvation can be defined as

$$\Delta = X_{\text{GY}}^{\text{S}} - X_{\text{GY}}^{\text{0}} = \frac{(\nu_{\text{M}} - X_{\text{GY}}^{\text{0}}\nu_{\text{GY}} - X_{\text{DMF}}^{\text{0}}\nu_{\text{DMF}})}{(\nu_{\text{GY}} - \nu_{\text{DMF}})} \quad (4)$$

where X_{GY}^{0} and $X_{\text{DMF}}^{\text{0}}$ are the bulk molar fractions of GY and DMF, respectively. Thus, the Δ parameter can be used to quantify the preferential solvation being $\Delta = 0$ if there is no preferential solvation, that is, if the molar fraction of GY in the bulk is the same as the molar fraction of GY in the QB solvation shell.

As Figure 1B shows, the H-bond interaction plays a key role in the QB preferential solvation by GY, thus we introduce eq 5 to

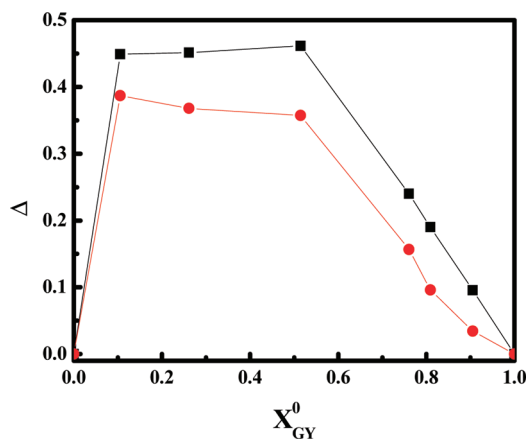


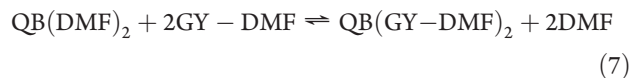
Figure 2. Δ values as a function of X_{GY}^{0} for QB in the GY:DMF mixture. (●) Δ calculated using eq 4; (■) Δ calculated using eq 5. $[\text{QB}] = 1 \times 10^{-4}$ M.

quantify the preferential solvation, where the Δ parameter is defined on the basis of the $\text{Abs}B_2/\text{Abs}B_1$ ratio.

$$\Delta = X_{\text{GY}}^{\text{S}} - X_{\text{GY}}^{\text{0}} = \frac{(r_{\text{M}} - X_{\text{GY}}^{\text{0}}r_{\text{GY}} - X_{\text{DMF}}^{\text{0}}r_{\text{DMF}})}{(r_{\text{GY}} - r_{\text{DMF}})} \quad (5)$$

where r_{M} , r_{GY} , and r_{DMF} are the $\text{Abs}B_2/\text{Abs}B_1$ ratio values for QB in the solvent mixtures and in pure GY and DMF, respectively.

Figure 2 shows the Δ value as a function of X_{GY}^{0} for QB in the GY:DMF mixtures. As it can be observed, Δ goes through a maximum when X_{GY}^{0} is around 0.5 when the parameter is defined as eq 4 or eq 5. From Figure 2 it is evident the predominant role of the QB–GY:DMF H-bond interaction in the QB’s preferential solvation because the Δ_{max} value is larger when the parameter is defined by eq 5. Notice that the H-bond interaction is so strong that there is preferential solvation in the whole X_{GY}^{0} range and, consequently, Δ is zero only at $X_{\text{GY}}^{\text{0}} = 0$ and 1. Thus, QB–GY:DMF interaction seems to be the stronger in comparison with QB–DMF, QB–GY, GY–GY, and DMF–DMF interactions. One question that may arise is the role that the GY–DMF H-bonded species plays in the QB preferential solvation. This can be answered considering the preferential solvation model based on the two-step exchange model first proposed by Skwierczynski and Connors,⁵² and successfully applied to many different binary mixtures.⁵³ Equations 6 and 7 show the model adapted to our system:



Hence in this model, the two solvents interact to yield a common structure, GY–DMF H-bonded species. Then the probe, QB, solvated by DMF, GY, and the GY–DMF H-bonded species is represented by QB (DMF)₂, QB (GY)₂, and QB (GY–DMF)₂, respectively. It should be noted that, although any number of solvent molecules could be exchanged, the best fits were obtained using two molecules, similar to what was found for several other solvent mixtures with $E_{\text{T}}(30)$.⁵³

Table 1. Parameters of QB in GY:DMF Binary Mixture in Homogeneous Media and in AOT RMs^a

	E_T^{DMF}	E_T^{GY}	$E_T^{\text{GY-DMF}}$	$f_{\text{GY/DMF}}$	$f_{\text{GY-DMF/DMF}}$	corr. coeff.
homogeneous media	42.23	58.60	52.35	17.44	22.02	0.9992
$W_s = 2$	48.40	58.23	54.74	3.29	6.98	0.9997

^a [AOT] = 0.10 M; [QB] = 1×10^{-4} M.

Table 2. ¹HNMR Chemical Shifts for GY, DMF, and Different Mixtures in Homogeneous Media and in AOT RMs^a

	$\delta_a/$ ppm ^b	$\delta_b/$ ppm ^c	$\delta_c/$ ppm ^d	$\delta_d/$ ppm ^e	$\delta_e/$ ppm ^f
Homogeneous Media					
GY	5.28	5.13			
DMF			8.04	2.97	2.79
GY:DMSO- <i>d</i> ₆ ($X_{\text{GY}}^0 = 0.10$)	4.58	4.49			
GY:DMF ($X_{\text{GY}}^0 = 0.12$)	4.71	4.61	8.04	2.96	2.79
GY:DMF ($X_{\text{GY}}^0 = 0.61$)	5.16	5.02	8.03	2.97	2.79
AOT RM $W_s = 2$					
GY-DMF ($X_{\text{GY}}^0 = 0.61$)	4.82	4.59	8.01	2.92	2.81
GY	4.81	4.60			

^a [AOT] = 0.10 M. ^{b,c} ¹HNMR GY chemical shifts for the primary and the secondary OH group, respectively. ^{d,e,f} ¹HNMR DMF chemical shifts for the H-C=O and the CH₃ groups, respectively.

The two solvent-exchange processes can be defined by two preferential solvation parameters, $f_{\text{GY/DMF}}$ and $f_{\text{GY-DMF/DMF}}$, which measure the tendency of the probe to be solvated by GY and the GY-DMF H-bonded species with respect to the solvation by DMF.

$$f_{\text{GY/DMF}} = \frac{\frac{X_{\text{GY}}^{\text{S}}}{X_{\text{DMF}}^{\text{S}}}}{\left(\frac{X_{\text{GY}}^0}{X_{\text{DMF}}^0}\right)^2} \quad (8)$$

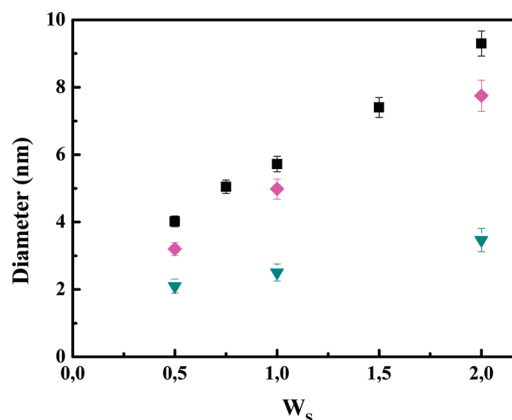
$$f_{\text{GY-DMF/DMF}} = \frac{\frac{X_{\text{GY-DMF}}^{\text{S}}}{X_{\text{DMF}}^{\text{S}}}}{\left(\frac{X_{\text{GY}}^0}{X_{\text{DMF}}^0}\right)^2} \quad (9)$$

where $X_{\text{GY-DMF}}^{\text{S}}$ is the mole fraction of the GY-DMF H-bonded species in the QB solvation sphere. All the other terms have the meaning described before.

The E_T^{M} of the mixed solvents is calculated as an average of the parameters values of the solvents GY, DMF, and GY-DMF in the sphere of solvation of the probe.

$$E_T^{\text{M}} = X_{\text{GY}}^{\text{S}} E_T^{\text{GY}} + X_{\text{DMF}}^{\text{S}} E_T^{\text{DMF}} + X_{\text{GY-DMF}}^{\text{S}} E_T^{\text{GY-DMF}} \quad (10)$$

From eqs 8–10, a general equation relating the E_T^{M} values of the binary mixture to the E_T values of the pure solvents, the preferential solvation parameters, and the solvent composition

**Figure 3.** Diameter values (nm) of GY:DMF/AOT/*n*-heptane RMs varying W_s at different X_{GY}^0 : (▼) 0.00; (■) 0.51; (◆) 1.00. [AOT] = 0.10 M.

can be derived as follows:

$$E_T^{\text{M}} = \left(E_T^{\text{DMF}} (1 - X_{\text{GY}}^0)^2 + E_T^{\text{GY}} f_{\text{GY/DMF}} (X_{\text{GY}}^0)^2 + E_T^{\text{GY-DMF}} f_{\text{GY-DMF/DMF}} (X_{\text{GY}}^0 X_{\text{GY}}^0) / (1 - X_{\text{GY}}^0)^2 + f_{\text{GY/DMF}} (X_{\text{GY}}^0)^2 + f_{\text{GY-DMF/DMF}} (X_{\text{GY}}^0 X_{\text{GY}}^0) \right) \quad (11)$$

The plot of E_T^{M} values as a function of X_{GY}^0 (Figure 1A) was fitted through a nonlinear regression to eq 11. Very good fit was obtained, and the results are displayed in Table 1. We observe that the value of $f_{\text{GY/DMF}}$ is much greater than 1, indicating strong preferential solvation by GY. Moreover, the even higher value of $f_{\text{GY-DMF/DMF}}$ means that QB is also largely solvated by the GY-DMF H-bonded species formed by the 1:1 interaction of GY with DMF. This behavior has been observed for other indicators in binary mixtures of DMF with alcohols.⁵³

In addition to the QB spectroscopic data, we used ¹HNMR to analyze the GY:DMF mixture. Table 2 shows the ¹HNMR chemical shifts for the different protons in pure GY and DMF, and at two GY:DMF compositions. Also, the values for GY: DMSO-*d*₆ (deuterated dimethyl sulfoxide) were included for comparison, since in this mixture GY has its hydrogen bond network broken. In every system studied, GY shows the peaks corresponding to the OH groups: the primary (H_a) and the secondary one (H_b).¹⁸ On the other hand, DMF spectra show the three proton signals corresponding to the H-C=O (H_c) and the CH₃ groups (H_d, H_e). It is clear from the data that the H-bond interaction between GY-GY is broken in the GY:DMF mixture, because the GY's δ 's shift to higher fields as the DMF content increases (i.e., lower X_{GY}^0). This is comparable to the effect observed in the GY:DMSO-*d*₆ mixture. As can be seen for X_{GY}^0 larger than 0.5, GY interacts through H-bonds to other GY molecules (GY-GY interactions), and the δ parameter tends to the pure GY value. On the other hand, and as expected, the DMF's signal remains practically constant in every system studied.

Having studied the GY:DMF mixture in homogeneous media, we extend our investigation to see the effect that a constrained environment has on the GY-DMF interactions. Thus, knowing the dramatic changes that the bulk polar solvents structure

experiences upon encapsulation by surfactants to form RMs,^{1,3,30} we want to obtain information about how the confinement can affect the bulk GY–DMF properties studying the GY:DMF mixture in AOT RMs media. To the best of our knowledge, there are no reports in the literature that explore this interesting and important effect.

GY:DMF/AOT/*n*-Heptane RMs. DLS Studies. DLS is used to assess whether the different GY:DMF mixtures are encapsulated by AOT to create RM media, because it is a powerful technique to evaluate the formation of these organized systems.^{1–3,6,20,21,54,55} Thus, if the mixture is really encapsulated to form RMs, the droplets size must increase as the W_s value increases with a linear tendency (swelling law of RMs), as is well established for water or polar solvent/surfactant RM systems.^{1,6,20} This feature can also demonstrate that the GY:DMF/AOT RM media consist of discrete spherical and noninteracting droplets of the mixture stabilized by the surfactant.²¹ On the other hand, if the GY:DMF mixture is not encapsulated by the surfactant, the droplet sizes should be insensitive or decrease with the polar solvent addition.²¹

In Figure 3 we report the droplets size values obtained in GY:DMF ($X_{GY}^0 = 0.51$)/AOT/*n*-heptane, GY/AOT/*n*-heptane, and DMF/AOT/*n*-heptane RMs. Similar results were obtained for the other GY:DMF (X_{GY}^0) composition investigated (not shown). In all the systems studied, it can be observed that there is an increase in the droplets size when the W_s value increases. The linear tendency observed in Figure 3 shows that all the polar solvents, including the GY:DMF mixtures are encapsulated in the polar core, yielding RMs that consist of discrete and noninteracting spherical droplets, in the sense of nonpercolated and/or fused systems where the RM droplet identity is lost.³ Also, we want to stress that the droplet sizes obtained through DLS for these AOT RMs do not depend on the AOT concentration, which also demonstrates that there is no droplet–droplet interaction, at least in the concentration range used. It must be noted that the GY/AOT and the DMF/AOT RMs have been studied in a recent communication.³¹

A peculiar result can be observed from Figure 3. The GY:DMF/AOT RM droplet sizes at any X_{GY}^0 value studied (not shown) are similar to the pure GY/AOT RMs independent of the DMF content, and larger than the one corresponding to the DMF/AOT RMs. We have recently demonstrated using DLS³¹ that the polar solvent–AOT interactions, especially the H-bond, are the key for the RM droplet size control. Since GY molecules are strongly bound to the AOT sulfonate group, as is shown by FT-IR,³⁰ it is possible that the H-bond interaction between GY and the AOT polar headgroup leads to an increase in the effective surfactant headgroup area (a), as is well established for AOT in isooctane/AOT/water RMs.⁵⁶ Maitra demonstrated that the AOT's a value increases from 36 to 51 Å² as the $W_0 = [H_2O]/[AOT]$ value increases from 4 to 20 because the water molecules bind to the AOT polar headgroup at the RM interface.⁵⁶ It is known that the RM droplet sizes depend, among many other variables, on the effective packing parameter of the surfactants, v/al_c , in which v and l_c are the volume and the length of the hydrocarbon chain, respectively, and a is the surfactant headgroup area. The RM sizes are larger when the surfactant packing parameter values are smaller.^{57,58} Thus, as the W_s values increase, GY binds to the AOT SO₃[−] group at the RM interfaces, increasing the surfactants' a values with a consequent decrease in the surfactant packing parameter and increase in the RM droplet size. This result evidences, as previously found,³¹ that the RMs droplet sizes depend strongly on the kind of interactions that the

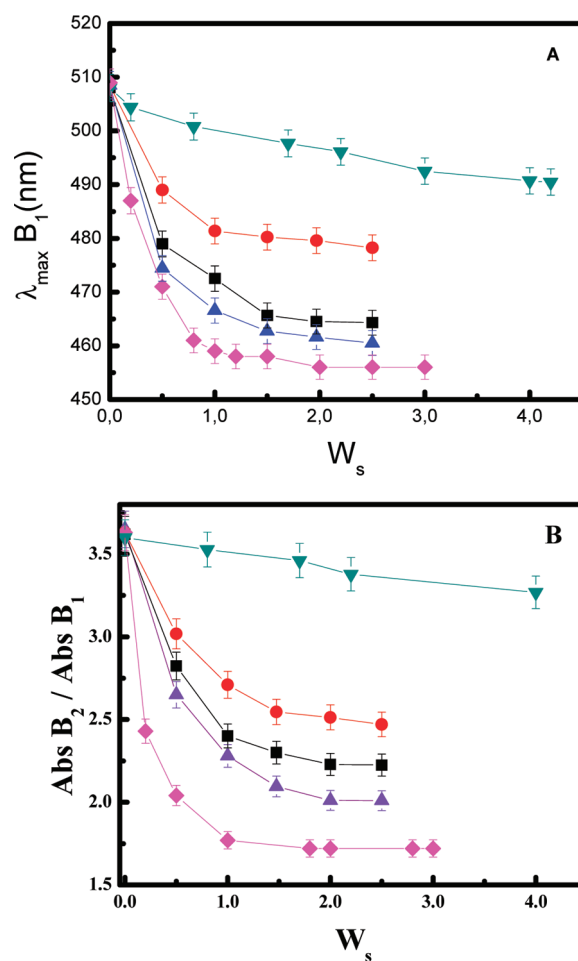


Figure 4. (A) Variation of $\lambda_{\max} B_1$ and (B) $\text{Abs} B_2 / \text{Abs} B_1$ ratio values as a function of W_s for QB in GY:DMF/AOT/*n*-heptane RMs at different X_{GY}^0 : (▼) 0.00; (●) 0.20; (■) 0.51; (▲) 0.79; (◆) 1.00. [AOT] = 0.10 M.

different polar solvents can make with the surfactant rather than their molar volume, even when a solvent mixture is confined at a nanoscale size.

¹H NMR Studies. The binary mixtures in AOT RMs were also studied using the noninvasive technique ¹H NMR. Figure S2 shows a representative ¹H NMR spectrum for the GY:DMF/AOT/*n*-heptane at $W_s = 2$ and $X_{GY}^0 = 0.50$. Table 2 shows the chemical shifts for GY and DMF protons of the GY:DMF mixture ($X_{GY}^0 = 0.61$) at $W_s = 2$. Similar results were obtained for $X_{GY}^0 = 0.20$ and 0.5 (results not shown). The data shows that the H-bond between GY–GY and GY–DMF is broken inside the AOT RMs media at these low W_s values. The δ values of GY are lower than the corresponding value at the same X_{GY}^0 in homogeneous media. It is interesting to note that these values perfectly match those obtained in GY/AOT/*n*-heptane RMs at $W_s = 2$ (Table 2). It seems that the strong H-bond interaction between GY and the AOT polar head is much stronger than the GY:DMF interaction in the mixture. Therefore, GY and DMF in the GY:DMF mixture encapsulated in the polar core of the AOT RMs behave as non-H-bond interacting solvents, as suggested using DLS. Similar results were found for the FA–water mixture encapsulated in AOT RMs.²⁵

On the other hand, the DMF's δ values shift a little upfield in comparison with the values obtained in bulk DMF. These shifts

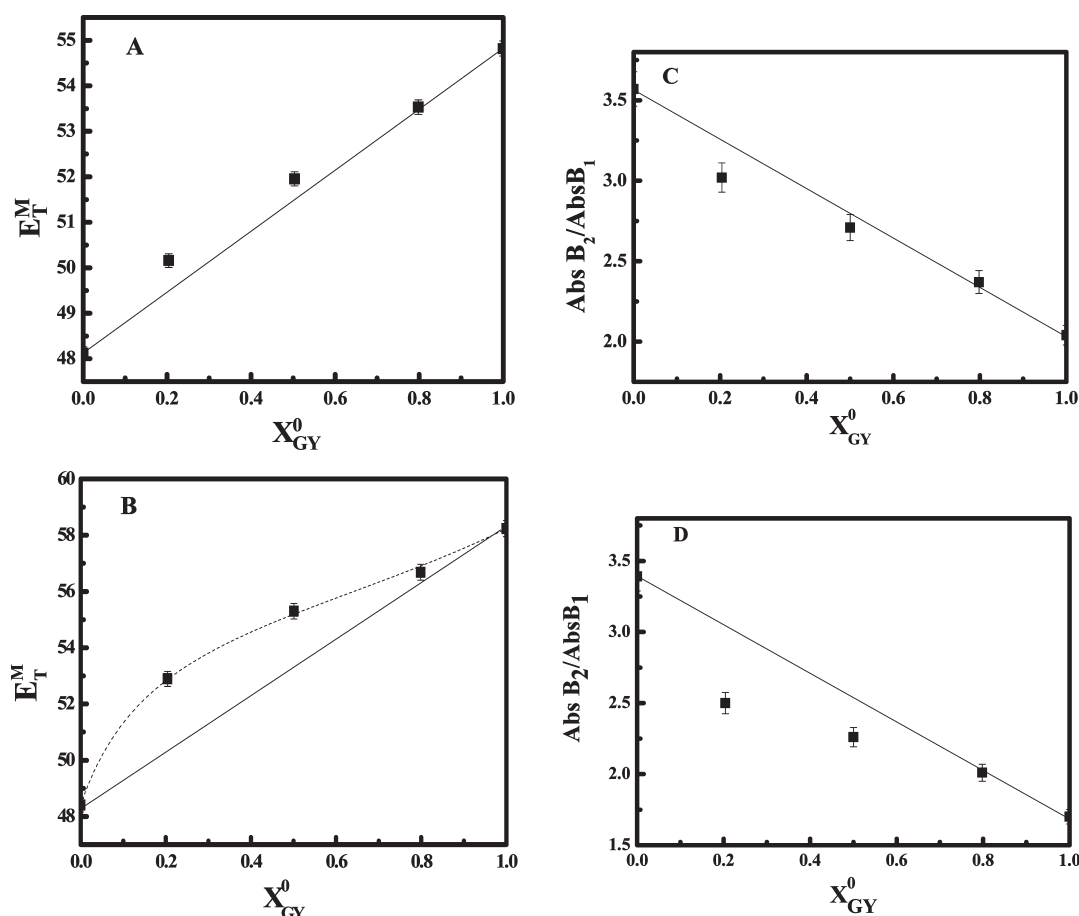


Figure 5. (A) E_T^M values for QB in GY:DMF/AOT/*n*-heptane RMs as a function of X_{GY}^0 at $W_s = 0.5$. (B) Experimental E_T^M values and fitted curve with eq 11 (dashed line) for QB in GY:DMF/AOT/*n*-heptane RMs as a function of X_{GY}^0 at $W_s = 2.0$. (C) $Abs B_2/Abs B_1$ values for QB in GY:DMF/AOT/*n*-heptane RMs as a function of X_{GY}^0 at $W_s = 0.5$. (D) $Abs B_2/Abs B_1$ ratio values for QB in GY:DMF/AOT/*n*-heptane RMs as a function of X_{GY}^0 at $W_s = 2.0$. $[AOT] = 0.10$ M. The straight lines were plotted to guide the eye; they represent no preferential solvation of QB by the mixture.

probably reflect the fact that DMF complexes with the Na^+ ions through their carbonyl and nitrogen groups.³⁰ It is known that DMF have a large affinity for solvating cations^{59,60} as demonstrated by the preferential solvation of Na^+ by DMF in Water:DMF mixtures.^{61–65} IR, Raman, and NMR studies show that ions dissolved in DMF induce structure in the liquids, suggesting that their oxygen atoms interact with the cations.^{66–69}

Studies Using QB as a Molecular Probe. In the homogeneous media we have demonstrated that QB is a strong hydrogen bond acceptor molecule that is preferentially solvated mostly by GY–DMF H-bonded species in the GY:DMF mixture mainly due to H-bond interaction.

Previous studies^{14,45} have been shown that QB exists at the AOT RMs interface in water and nonaqueous AOT RMs at any polar solvent content. Thus, we are confident that QB will monitor the changes at the AOT interface properties.

Figure 4A,B shows the $\lambda_{max} B_1$ and the $Abs B_2/Abs B_1$ ratio values for QB in GY:DMF/AOT/*n*-heptane RM varying W_s at $[AOT] = 0.10$ M and, at different X_{GY}^0 values, respectively. The results show a dramatic decrease in the $\lambda_{max} B_1$ and the $Abs B_2/Abs B_1$ ratio values as W_s increases at any X_{GY}^0 studied, indicating that QB senses a more polar H-bond donor environment as W_s increases. It is worth noting that the tendency of $\lambda_{max} B_1$ and the $Abs B_2/Abs B_1$ is similar to the one found when only GY is encapsulated, at any

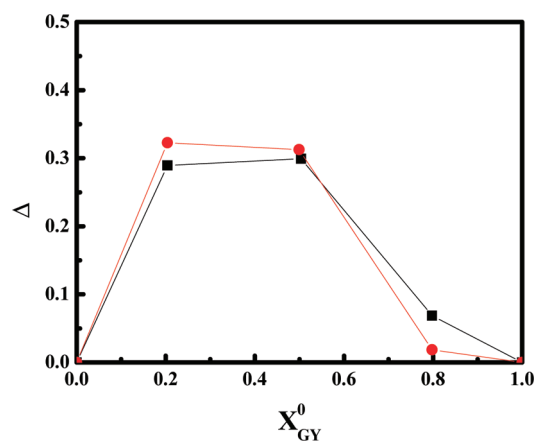


Figure 6. Δ values as a function of X_{GY}^0 for QB in GY:DMF/AOT/*n*-heptane RMs at $W_s = 2.0$. (■) Δ calculated using eq 4; (●) Δ calculated using eq 5. $[AOT] = 0.10$ M.

X_{GY}^0 studied. Figure 5A,B shows E_T^M values for QB in GY:DMF/AOT/*n*-heptane RMs as a function of X_{GY}^0 at $W_s = 0.5$ and 2.0, respectively, while Figure 5C,D shows the QB's $Abs B_2/Abs B_1$ ratio values as a function of X_{GY}^0 at $W_s = 0.5$ and 2.0, respectively.

As it can be observed from Figure 5A,B at $W_s = 0.5$, there is very little deviation from the linearity of the plots below $X_{GY}^0 = 0.5$. After that, the plot is linear with the GY molar fraction. The results suggest that the H-bond interaction between GY and DMF inside AOT RMs dramatically decreases in comparison with the homogeneous mixture (Figure 1A,B) being the solvation of QB almost ideal. Furthermore, because the tendency observed in the $\lambda_{\max} B_1$ and the Abs B_2 /Abs B_1 ratio values shown in Figure 4A,B, we suggest that at $W_s = 0.5$, where the polar solvent–AOT interaction is large, QB only detects GY molecules at the interface as DLS and ^1H NMR experiments suggest.

On the other hand, the situation is quite different at $W_s = 2.0$. Figure 5B,D shows that there is a deviation from the linearity in the plots, showing that there is preferential solvation of QB in the AOT RMs media by the GY:DMF mixture, although in less magnitude than in homogeneous media.

In a way to quantify the preferential solvation observed in the RMs media at $W_s = 2.0$, we have calculated the values of Δ as a function of X_{GY}^0 using eqs 4 and 5 and plotted them in Figure 6. It is clear that Δ values obtained in the AOT RMs are smaller than the ones obtained in homogeneous media (Figure 2).

Furthermore we have fitted the plot of E_T^M as a function of X_{GY}^0 to eq 11 at $W_s = 2$ (Figure 5B) and the result is depicted in Table 1. As observed, the effects of the binary mixtures' encapsulation in the RMs polar core strongly diminish the preferential solvation parameters. Also, a dramatic drop of the $f_{\text{DMF-GY/DMF}}$ value can be seen in comparison with the value found in homogeneous media, a result that suggests that the GY–DMF H-bonded species solvates less QB through H-bond interaction at the AOT RMs interface because of the GY–AOT interaction.

The results found in the AOT RMs can be explained considering the different kind of interactions between the polar solvents and the AOT polar headgroup. It is known that the GY–AOT interaction (H-bond) is very strong, even stronger than the water–AOT one.^{14,18,30} Also, it has been demonstrated that all GY molecules interact with the AOT polar headgroup and the counterions at the interface, even at the maximum W_s value that the system can accept ($W_s \sim 4$). Hence, practically no free GY molecules are found in the polar core.^{14,18,30} On the other hand, as previously shown, DMF interacts mainly with the Na^+ counterions.³⁰ Thus, it seems that GY–AOT interaction is so strong that GY molecules no longer interact with the DMF molecules when the GY:DMF mixture is encapsulated inside the AOT RMs, particularly at low W_s values.

CONCLUSIONS

We have demonstrated using UV–visible absorption, ^1H NMR spectroscopies, and DLS technique how the confinement environment can dramatically affect the interaction between two different solvents: GY and DMF. In homogeneous media, GY and DMF interact strongly through H-bond interactions, while the opposite is found when the mixture is encapsulated inside AOT RMs. Herein and because of the strong GY–AOT interaction, when the GY–DMF mixture is encapsulated in the polar core of the AOT RMs, GY binds through a H-bond to the AOT SO_3^- group at the interface, and DMF makes complexes with the Na^+ counterions in the polar core of the aggregates, significantly diminishing the GY–DMF interaction. Therefore, each solvent (in the mixture) behaves as noninteracting solvents inside the RM media, especially at low W_s values. In this way, we would like

to emphasize that results found in an homogeneous environment can not always be extrapolated to confined media such as RMs. Moreover, the molecular probe QB at the AOT RM interface can interact almost exclusively with the GY molecules (more noticeable at low W_s values) and the preferential solvation detected in homogeneous media almost disappears inside the RMs.

Since RMs are an oversimplified model for the biological membrane, especially because the very large interfacial region provided by these systems can be expected to enhance some effects such as H-bond interactions, we think that the results give some insight on the interactions between H-bond donor solvents and peptide bonds.

ASSOCIATED CONTENT

S Supporting Information. Figure S1: QB absorption spectra in GY:DMF mixture. Figure S2: ^1H NMR spectrum for the GY:DMF/AOT/*n*-heptane at $W_s = 2$ and $X_{GY}^0 = 0.50$. This material is available free of charge via the Internet at <http://pubs.acs.org>.

AUTHOR INFORMATION

Corresponding Author

*E-mail: mcorrea@exa.unrc.edu.ar.

ACKNOWLEDGMENT

We gratefully acknowledge the financial support for this work by the Consejo Nacional de Investigaciones Científicas y Técnicas (CONICET), Agencia Córdoba Ciencia, Agencia Nacional de Promoción Científica y Técnica, and Secretaría de Ciencia y Técnica de la Universidad Nacional de Río Cuarto. J.J.S., N.M.C., and R.D.F. hold research positions at CONICET. A.M. D. thanks CONICET for a research fellowship.

REFERENCES

- (1) Silber, J. J.; Biasutti, M. A.; Abuin, E.; Lissi, E. *Adv. Colloid Interface Sci.* **1999**, *82*, 189.
- (2) De, T. K.; Maitra, A. *Adv. Colloid Interface Sci.* **1995**, *59*, 95.
- (3) Moulik, S. P.; Paul, B. K. *Adv. Colloid Interface Sci.* **1998**, *78*, 99.
- (4) Martino, A.; Kaler, E. W. *J. Phys. Chem.* **1990**, *94*, 1627.
- (5) Ray, S.; Moulik, S. P. *Langmuir* **1994**, *10*, 2511.
- (6) Fletcher, P. D. I.; Galal, M. F.; Robinson, B. H. *J. Chem. Soc., Faraday Trans. I* **1984**, *80*, 3307.
- (7) Fletcher, P. D. I.; Grice, D. D.; Haswell, S. J. *Phys. Chem. Chem. Phys.* **2001**, *3*, 1067.
- (8) Friberg, S. E.; Liang, P. *Colloid Polym. Sci.* **1986**, *264*, 449.
- (9) Rico, I.; Lattes, A. *J. Colloid Interface Sci.* **1984**, *102*, 285.
- (10) Arcoleano, V.; Aliotta, F.; Goffredi, M.; La Manna, G.; Turco Liveri, V. *Mater. Sci. Eng., C* **1997**, *5*, 47.
- (11) Mathew, C.; Saidi, Z.; Peyrelasse, J.; Boned, C. *Phys. Rev. A* **1991**, *43*, 873.
- (12) Lopez-Cornejo, P.; Costa, S. M. B. *Langmuir* **1998**, *14*, 2042.
- (13) Laia, C. A. T.; Lopez-Cornejo, P.; Costa, S. M. B.; d'Oliveira, J.; Martinho, J. M. G. *Langmuir* **1998**, *14*, 3531.
- (14) Falcone, R. D.; Correa, N. M.; Biasutti, M. A.; Silber, J. J. *Langmuir* **2000**, *16*, 3070.
- (15) Silber, J. J.; Falcone, R. D.; Correa, N. M.; Biasutti, M. A.; Abuin, E.; Lissi, E.; Campodonico, P. *Langmuir* **2003**, *19*, 2067.
- (16) Novaki, L. P.; Correa, N. M.; Silber, J. J.; El Seoud, O. A. *Langmuir* **2000**, *16*, 5573.
- (17) Falcone, R. D.; Correa, N. M.; Biasutti, M. A.; Silber, J. J. *J. Colloid Interface Sci.* **2006**, *296*, 356.

- (18) El Seoud, O. A.; Correa, N. M.; Novaki, L. P. *Langmuir* **2001**, *17*, 1847.
- (19) Shirota, H.; Segawa, H. *Langmuir* **2004**, *20*, 329.
- (20) Riter, R. E.; Undiks, E. P.; Kimmel, J. R.; Levinger, N. E. *J. Phys. Chem. B* **1998**, *102*, 7931.
- (21) Riter, E. R.; Kimmel, J. R.; Undiks, E. P.; Levinger, N. E. *J. Phys. Chem. B* **1997**, *101*, 8292.
- (22) Raju, B. B.; Costa, S. M. B. *Spectrosc. Acta, Part A* **2000**, *56*, 1703.
- (23) Laia, C. A. T.; Brown, W.; Almgrem, M.; Costa, S. M. B. *Langmuir* **2000**, *16*, 8763.
- (24) Laia, C. A. T.; Costa, S. M. B. *Langmuir* **2002**, *18*, 1494.
- (25) Correa, N. M.; Pires, P. A. R.; Silber, J. J.; El Seoud, O. A. *J. Phys. Chem. B* **2005**, *109*, 21209.
- (26) Atay, N. Z.; Robinson, B. H. *Langmuir* **1999**, *15*, 5026.
- (27) Hayes, D. G.; Gulari, E. *Langmuir* **1995**, *11*, 4695.
- (28) Novaira, M.; Moyano, F.; Biasutti, M. A.; Silber, J. J.; Correa, N. M. *Langmuir* **2008**, *24*, 4637.
- (29) Correa, N. M.; Levinger, N. E. *J. Phys. Chem. B* **2006**, *110*, 13050.
- (30) Durantini, A. M.; Falcone, R. D.; Silber, J. J.; Correa, N. M. *ChemPhysChem* **2009**, *10*, 2034.
- (31) Falcone, R. D.; Silber, J. J.; Correa, N. M. *Phys. Chem. Chem. Phys.* **2009**, *11*, 11096.
- (32) Sengwa, R. J.; Khatri, V.; Sankhla, S. *Fluid Phase Equilib.* **2008**, *266*, 54.
- (33) Ziolkiewicz, J. *Phys. Chem. Chem. Phys.* **2000**, *2*, 2925.
- (34) Santo, M.; Anunziata, J. D.; Cattana, R.; Silber, J. J. *Spectrochim. Acta, A* **1995**, *51*, 1749.
- (35) Reichardt, C. *Solvent and Solvent Effects in Organic Chemistry*, 2nd ed.; VCH: New York NY, 1990.
- (36) Davis, D. M.; Mcloskey, D.; Birch, D. J. S.; Gellert, P. R.; Kittlety, R. S.; Swart, R. M. *Biophys. Chem.* **1996**, *60*, 63.
- (37) Falcone, R. D.; Biasutti, M. A.; Correa, N. M.; Silber, J. J.; Lissi, E.; Abuin, E. *Langmuir* **2004**, *20*, 5732.
- (38) Biasutti, M. A.; Abuin, E. A.; Silber, J. J.; Correa, N. M.; Lissi, E. A. *Adv. Colloid Interface Sci.* **2008**, *136*, 1.
- (39) Moyano, F.; Falcone, R. D.; Mejuto, J. C.; Silber, J. J.; Correa, N. M. *Chem.—Eur. J.* **2010**, *16*, 8887.
- (40) Xu, L.; Hu, X.; Lin, R. *J. Solution Chem.* **2003**, *32*, 363.
- (41) Palecz, B.; Piekarski, H. *J. Solution Chem.* **1997**, *26*, 621.
- (42) Paola, G. D.; Belleau, B. *Can. J. Chem.* **1977**, *55*, 3825.
- (43) Yu, L.; Zhu, Y.; Hu, X.-G.; Pang, X.-H. *J. Chem. Eng. Data* **2006**, *51*, 1110.
- (44) Ueda, M.; Schelly, Z. A. *Langmuir* **1989**, *5*, 1005.
- (45) Correa, N. M.; Biasutti, M. A.; Silber, J. J. *J. Colloid Interface Sci.* **1995**, *172*, 71.
- (46) Correa, N. M.; Biasutti, M. A.; Silber, J. J. *J. Colloid Interface Sci.* **1996**, *184*, 570.
- (47) Dimroth, K.; Reichardt, C.; Siepmann, T.; Bohlmann, F. *Ann. Chem.* **1963**, *661*, 1.
- (48) Marcus, Y. *Chem. Soc. Rev.* **1993**, 409.
- (49) Cattana, R.; Silber, J. J.; Anunziata, J. *Can. J. Chem.* **1992**, *70*, 2677.
- (50) Rao, D. M.; Kalidas, C. *J. Chem. Eng. Data* **1990**, *35*, 8.
- (51) Chatterjee, P.; Bagchi, S. *J. Chem. Soc., Faraday Trans.* **1991**, *87*, 587.
- (52) Skwierczynski, R. D.; Connors, A. J. *Chem. Soc., Perkin Trans 2* **1994**, *3*, 467.
- (53) (a) Roses, M.; Rafols, C.; Ortega, J.; Bosch, E. *J. Chem. Soc., Perkin Trans. 2* **1995**, 1607. (b) Herodes, K.; Leito, I.; Koppel, I.; Roses, M. *J. Phys. Org. Chem.* **1999**, *12*, 109. (c) Bevilaqua, T.; da Silva, D. C.; Machado, V. G. *Spectrochim. Acta, Part A* **2004**, *60*, 951. (d) Bevilaqua, T.; Goncalves, T. F.; Venturini, C. D. G.; Machado, V. G. *Spectrochim. Acta, Part A* **2006**, *65*, 535. (e) do R. Silva, M. A.; da Silva, D. C.; Machado, V. G.; Longhinotti, E.; Frescura, V. L. A. *J. Phys. Chem. A* **2002**, *106*, 8820.
- (54) Eastoe, J.; Gold, S.; Rogers, S. E.; Paul, A.; Welton, T.; Heenan, R. K.; Grillo, I. *J. Am. Chem. Soc.* **2005**, *127*, 7302.
- (55) Gao, Y.; Li, N.; Zheng, L.; Bai, X.; Yu, L.; Zhao, X.; Zhang, J.; Zhao, M.; Li, Z. *J. Phys. Chem. B* **2007**, *111*, 2506.
- (56) Maitra, A. *J. Phys. Chem.* **1984**, *88*, 5122.
- (57) Li, Q.; Li, T.; Wu, J. *J. Colloid Interface Sci.* **2001**, *239*, 522.
- (58) Evans, D. F.; Ninham, B. W. *J. Phys. Chem.* **1986**, *90*, 226.
- (59) Puhovski, Y. P.; Safanova, L. P.; Rode, B. M. *J. Mol. Liquid* **2003**, *103–104*, 15.
- (60) Barthel, J.; Buchner, R.; Wurm, B. *J. Mol. Liquid* **2002**, *98–99*, 51.
- (61) Criss, C. M.; Luksha, E. *J. Phys. Chem.* **1968**, *72*, 2966.
- (62) Kobara, H.; Wakisaka, A.; Takeuchiibusuki, K. T. *J. Phys. Chem. B* **2003**, *107*, 11827.
- (63) Alves, W. A.; Tellez Soto, C. A.; Hollauer, E.; Faria, R. B. *Spectrochim. Acta A* **2005**, *62*, 755.
- (64) Marcus, Y. *Pure Appl. Chem.* **1990**, *62*, 978.
- (65) Holz, M.; Rau, C. K. *J. Chem. Soc., Faraday Trans. 1* **1982**, *78*, 1899.
- (66) Akhter, M. S.; Alawi, S. M. *Colloids Surf, A* **2003**, *219*, 281.
- (67) Hirota, E.; Sugisaki, R.; Nielsen, C. J.; Sorensen, G. O. *J. Mol. Spectrosc.* **1974**, *49*, 251.
- (68) Gardiner, D. J.; Lees, J. A.; Straughan, B. P. *J. Mol. Struct.* **1979**, *53*, 15.
- (69) Lees, J. A.; Straughan, B. P.; Gardiner, D. J. *J. Mol. Struct.* **1981**, *71*, 61.